Molecular Crystals and Liquid Crystals Science and Technology. Section A. Molecular Crystals and Liquid Crystals

Publication details, including instructions for authors and subscription information:
http://www.tandfonline.com/loi/gmcl19

Dielectric Relaxations of a Smectic Side-Chain Liquid-Crystalline Polymer in Different Alignment States

Z. Z. Zhong [a] , W. L. Gordon [a] , D. E. Schuele [a] , R. B. Akins [b] & V. Percec [c]

[a] Department of Physics, Case Western Reserve University, Cleveland, OH, 44106-7079, U.S.A.

[b] Liquid Crystal Institute, Kent State University, Kent, OH, 44242-0001, U.S.A.

[c] Department of Macromolecular Science, Case Western Reserve University, Cleveland, OH, 44106-7202, U.S.A.

Version of record first published: 04 Oct 2006.

To cite this article: Z. Z. Zhong , W. L. Gordon , D. E. Schuele , R. B. Akins & V. Percec (1994): Dielectric Relaxations of a Smectic Side-Chain Liquid-Crystalline Polymer in Different Alignment States, Molecular Crystals and Liquid Crystals Science and Technology. Section A. Molecular Crystals and Liquid Crystals, 238:1, 129-145

To link to this article: http://dx.doi.org/10.1080/10587259408046922

Mol. Cryst. Liq. Cryst., 1994, Vol. 238, pp. 129–145
Reprints available directly from the publisher
Photocopying permitted by license only

Printed in the United States of America

Dielectric Relaxations of a Smectic Side-Chain Liquid-Crystalline Polymer in Different Alignment States

Z. Z. ZHONG, W. L. GORDON and D. E. SCHUELE

Department of Physics, Case Western Reserve University, Cleveland, OH 44106-7079, U.S.A.

and

R. B. AKINS

Liquid Crystal Institute, Kent State University, Kent, OH 44242-0001, U.S.A.

and

V. PERCEC

Department of Macromolecular Science, Case Western Reserve University, Cleveland, OH 44106-7202, U.S.A.

(Received October 1, 1992; in final form April 22, 1993)

The complex dielectric constant has been measured for a polyvinyl-ether based cyano-biphenyl side-chain liquid-crystalline polymer over the temperature range of 100–400 K and frequency range of $10-10^5$ Hz. In the smectic-A phase, both homogeneous and homeotropic alignments were achieved with a 7-Tesla magnetic field by slowly cooling the samples down from the isotropic phase to room temperature. The low-frequency δ loss peaks are suppressed in the homogeneous state and enhanced in the homeotropic state while high-frequency α loss peaks are enhanced in the homogeneous and almost absent in the homeotropic. The Arrhenius plot of each process shows a rapid decrease in the relaxation frequency as the temperature approaches T_g, which may somehow reflect the glassy behavior of the polymer backbone and has been analyzed by WLF and Vogel-Fulcher equations. The results from two samples with different degree of polymerization are compared in terms of T_g.

Keywords: side-chain liquid-crystalline polymer, dielectric relaxation, glass transition, polymer backbone, smectic-A liquid crystal, Fuoss-Kirkwood function, WLF equation, Vogel-Fulcher equation, smectic side-chain

INTRODUCTION

Side-chain liquid-crystalline polymers (SCLCPs) have received wide attention since the first systematic synthesis in the late 70's.[1-4] A SCLCP system usually consists of a polymer backbone, or main chain, attached through some flexible carbon

"spacers" by liquid crystal (LC) mesogenic groups in the side chain to form a "comb-like" structure.[5] This structure combines polymer advantages (good film-forming and other mechanical properties) with electro-, magneto-optical properties in low molecular mass LCs. They are of considerable interest scientifically as hybrid-nature materials and technologically as potential media for a variety of applications in physical optics and display technology.[6,7] As films sandwiched between two conducting glass plates, they are promising for high-density optical data storages, for optical elements such as Fresnel zone plates or planar waveguides, or for nonlinear optical processing such as the second harmonic generation of laser light.[7,8] It is vital to investigate the molecular structures and molecular dynamics in such a polymer system and its packing information in the fluids, as well as its different macroscopically aligned configurations in LC states, i.e., homeotropic (H), planar (P) or homogeneous, and unaligned (U) orientations of side chain mesogens with respect to the plane of the film.[9,10]

A dielectric relaxation process in the frequency domain is equivalent to the Fourier transformation of a step-response in the time domain, which is basically a molecular dynamic process of some segments containing permanent or induced dipole moments in the material at a given equilibrium temperature.[11] Many dielectric measurements have been conducted on various kinds of thermotropic SCLCP samples.[12-25] At low temperature, usually below the glass transition T_g, SCLCPs are either semi-crystalline or glassy like most of conventional polymers in the solid state, whose locally-involved relaxation processes are often labeled as β, γ, etc. with decreasing temperature.[26] Above the solid-liquid transition temperatures, sometimes equal to T_g, they exhibit liquid crystalline mesophases, i.e., smectic, nematic, and isotropic, *et al.*, in which there are usually two relaxation processes in the neighborhood of T_g, being labeled δ and α.

To analyze the dielectric spectra in the mesogenic phases of the SCLCP system, some theories for low molecular mass LCs, such as rotational diffusion modes in nematics,[27-29] can be adapted. Although rotational field models of relaxation were developed for nematics, they are good approximation applicable to the dielectric relaxations in smectic-A (s_A) phase. This follows from a molecular point of view since the long range spatial periodicity characteristic of s_A phase plays no part in relaxing the dipole moments, although it will influence the internal field effect. Thus, on passing from the nematic to s_A phase, broad continuity would be expected with only slight changes in permittivities and relaxation rate.[10] This theoretical consideration is more valid when the SCLCP system is in the mesophase higher-temperature side closer to the isotropic temperature, or clearing point T_c. On the other hand, when the SCLCP samples are in the lower-temperature side closer to T_g, the molecular rotations of mesogenic group will be strongly correlated to the stiff polymer chain motion, resulting in the theoretical interpretations having to take into account the dipolar segments in both side chain and backbone.[30] Fortunately, in most cases, the relaxations due to the mesogenic group are more promising than those due to the backbone and just slow down rapidly as temperature approaches T_g from the LC phase. Hence, mesogenic relaxation processes may reflect the glassy behaviors of the polymer chain, which will, to some extent, be helpful in understanding the debated glass transition in polymeric materials.[31]

Cyano-biphenyl SCLCPs were first studied dielectrically by H. Kresse and co-workers, with the unaligned samples based on polyacrylates and polymethacrylates,[12] and polysiloxanes,[13] from which only one relaxation process was observed. C. M. Haws *et al.* did observe both δ and α processes in their unaligned GN/19 sample, however the main chain was a siloxane copolymer.[24]

In this paper, the dielectric measurements were conducted with two polyvinyl-ether based cyano-biphenyl SCLCP samples with carbon spacer length of 7, one having degree of polymerization (DP) of about 7.3 and the other 30, which are both in s_A phases at room temperature. The samples were successfully aligned both homeotropically and planarly in a 7-Tesla superconducting magnetic field by carefully slowly cooling down from the isotropic temperature to room temperature. In the H-aligned sample, the low-frequency δ-peaks are enhanced dramatically compared with the unaligned while the high-frequency α-peaks are completely absent. In contrast, the δ-peaks are suppressed while α-peaks are enhanced in the P-alignment as compared with the unaligned sample. The data has been fitted to semi-empirical relaxation line shapes (Fuoss-Kirkwood) using nonlinear least squares minimization to distinguish these two processes with a subtracted DC conductivity. The Arrhenius plot, frequency maxima of each process vs. reciprocal temperature, shows typical glassy behaviors as temperature approaches to T_g from the mesophase range, which will be analyzed using the WLF and Vogel-Fulcher (VF) equations. The longer chain sample (DP ≈ 30), having a 8 K higher T_g than the shorter chain (DP ≈ 7.3), has basically the same relaxation processes as the shorter one, except the relaxation frequencies are about $10^{0.8}$ Hz lower than those in the shorter chain.

EXPERIMENT

The SCLCP samples, Poly{7-[(4-cyano-4′-biphenyl)oxy]heptyl vinyl ether}s, were synthesized using living cationic poymerization by V. Percec and M. Lee in an attempt to elucidate the molecular design mechanism in the side-chain system.[32] The chemical structure is shown in Scheme, which contain a cyano-biphenyl-oxy mesogen attached via seven carbon spacers (—CH_2—) to a vinyl-ether backbone. C7DP8, which was designed to have a DP of 8, has an average DP of 7.3 and C7DP30 has a DP of 30. At room temperature and 1 kHz frequency, the dielectric constant (ε′) is approximately 3.2 and the conductivity is 6.2×10^{-9} S/m for C7DP8; 2.8 and 1.7×10^{-9} S/m, respectively for C7DP30. Both samples are in s_A phase at room temperature, and were measured without further chemical treatment.

Differential scanning calorimetry (DSC) measurements were taken with a Dupont 910 cell base with Dupont 990 thermal analyzer at a 10 K/min heating rate. The phase transitions of the samples are summarized in Table I. The first DSC scanning with C7DP8 showed a semi-crystalline transition at 285 K, overlapping

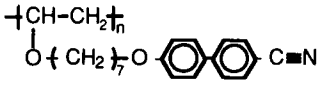

SCHEME Chemical structure of the studied cyano-biphenyl side-chain liquid crystalline polymer (SCLCP).

TABLE I

Phase transitions in the studied SCLCP samples from DSC scan at 10 K/min heating rate

Sample	$\bar{n}$ (DP)	phase transitions (K)	10^{-3}Mn
C7DP8	7.3	g 282 s_A 392 i	2.43
C7DP30	30	g 290 s_A 408 i	10.3

its glass transition at 282 K, which disappeared in subsequent scans. The glass transition of C7DP30 is 290 K, 8 K higher than C7DP8. The isotropic transition temperature (T_i) is 392 K for C7DP8 and 408 K for C7DP30.

The dielectric sample cell was constructed of two parallel ITO (Indium Tin Oxide, 20 Ω/□) glass plates, which allows for optical examination. The edge of the ITO plate was stripped using a solution of hydrochloric and nitric acids. The two plates were glued together by a high temperature epoxy, separated by a 25 μm kapton spacer, to form a parallel-plate capacitor with the empty cell capacitance C_0 of 7 pF. The SCLCP sample was inserted onto the cell through capillary action, being placed on a hot stage in a vacuum chamber and heated above the isotropic temperature. The casting time for C7DP8 was about 3 hours and slightly longer for C7DP30.

In order to identify the relaxation processes in terms of local molecular dynamic modes and to determine its dielectric anisotropy, the SCLCP sample has to be macroscopically aligned in either the homeotropic or the planar orientation states. The sample can be magnetically aligned since the mesogens in the side group have strong diamagnetic anisotropy. Both H- and P-alignments were achieved by slowly cooling the sample placed in a 7-Tesla superconducting magnet (Cryomagnetics, Inc.) from above the isotropic to room temperature. The cooling rate of 5 K/hour was well controlled by a Lakeshore temperature controller together with a custom-built ramp. For the H-alignment, the cell was mounted with its layer normal parallel to the field; for P-alignment, perpendicular to the field.

The dielectric loss (G/ω) and capacitance (C) were taken at 17 frequencies (10 Hz–100 kHz, in a linear log ratio) using a ratio arm transformer bridge[33] (CGA-83, C. Andeen and Assoc.) at 5 K interval temperature from 100 K to 400 K. For the aligned samples, the upper temperature was 370 K, well below the clearing points, to avoid possibly destroying the alignments. The bridge's oscillation voltage was chosen to be the lowest level (≈0.1 volts/rms) to avoid disturbing the LC's macroscopic alignment and inducing the additional dipole moments. The individual cell was placed in a cryostats for data acquisition at low temperatures and a vacuum oven for data collection at elevated temperatures. The temperature was controlled by a Lakeshore DRC 82C controller with two platinum sensors, which can stabilize temperature at 10 mK to meet the isothermal conditions. The data acquisition steps were controlled by a HP-87 computer through an IEEE 488 interface. The relationship between the complex dielectric constant (ε^*) and the measured capaci-

tance, C and loss, G/ω is given by the following, with empty cell capacitance C_0 and DC conductance G_{DC}.

$$\varepsilon^*(\omega) = \varepsilon'(\omega) - i\varepsilon''(\omega)$$
$$\varepsilon'(\omega) = C(\omega)/C_0 \quad (1)$$
$$\varepsilon''(\omega) = [G(\omega)/\omega - G_{DC}/\omega]/C_0$$

RESULTS

The dielectric spectrum of the SCLCP system in the whole temperature range ($T < T_i$) shows totally four relaxation processes. Figure 1 gives the dielectric loss of the unaligned C7DP8 at 10 Hz, 1 kHz, and 100 kHz. There are two relaxations below calorimetric T_g, labeled by β and γ with decreasing temperature. In the s_A region ($T_g < T < T_i$), it contains two typical processes in the SCLCP mesophase, labeled with δ and α with decreasing temperature. The isotropic temperature T_i, having a thermodynamic nature in mesophase transitions, appears to be independent of bridge frequency.

β and γ Relaxations

β and γ relaxations occur below the glass transition of the SCLCP sample, where the polymer chain is essentially frozen. These two low-temperature relaxations are very similar to those in poly{vinyl methyl ether}[34] and usually involve only local motions of some segments either in the main chain or in the side chain.[35] They are

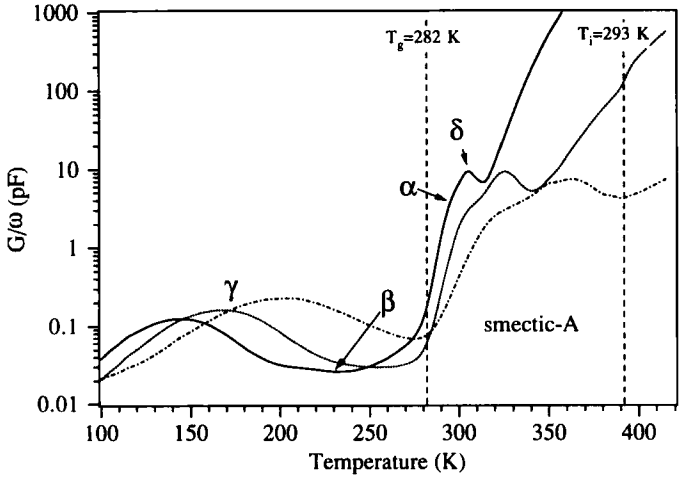

FIGURE 1 Dielectric loss overview for the unaligned C7DP8 at 10 Hz(——), 1 kHz (·····), and 100 kHz(-·-·-·-) as compared with its glass transition T_g and isotropic temperature T_i from DSC data. Four processes are labeled as δ, α, β, and γ in decreasing temperature.

almost independent of the different alignments and the degree of polymerization. Figure 2 shows the γ peaks of the unaligned C7DP8 from 145 K to 165 K, which are stronger and broader than β peaks. The loss amplitude in the γ relaxation increases with increasing temperature and the relaxation frequency at a given temperature is much higher than that in the β relaxation. The broad γ process may combine a few different local motions, including some in the cyano-biphenyl group[36] in the side chain, and has an activation energy of about 40 kJ/mole. The β peaks are merged with the α process at higher frequencies (>1 kHz), where the main glass transition of the polymer appears.

Two Major Relaxations—α and δ

In the s_A region, there two major dielectric relaxation processes, a broad, high-frequency α peak and a narrow, low-frequency δ peak. The real part (capacitance) and imaginary part (dielectric loss) of the unaligned C7DP8 are shown in Figure 3 from 310 K to 330 K, with the δ peaks being much stronger than the α peaks. Figure 4 shows the corresponding spectra in H- and P-aligned samples. In the H-alignment, the δ-peaks are enhanced dramatically compared with the unaligned while the α-peaks are completely absent. In contrast, the δ-peaks are suppressed while α-peaks are increased in the P-alignment. The longer chain sample C7DP30 basically shows the similar relaxation phenomena except a slowdown in the relaxation frequency at a given temperature as compared with C7DP8.

Fuoss-Kirkwood Data Fitting

In simple systems, dielectric spectra often contain a few relatively narrow peaks which are often well separated in temperature, and are readily interpreted. The samples in the present investigation, however, have spectra in which the individual peaks, though discernible, are broad and overlapped to the point that dielectric information (peak areas, widths and relaxation frequencies) is corrupted by the tails of the adjacent peaks. A major goal is to obtain the activation energy for each

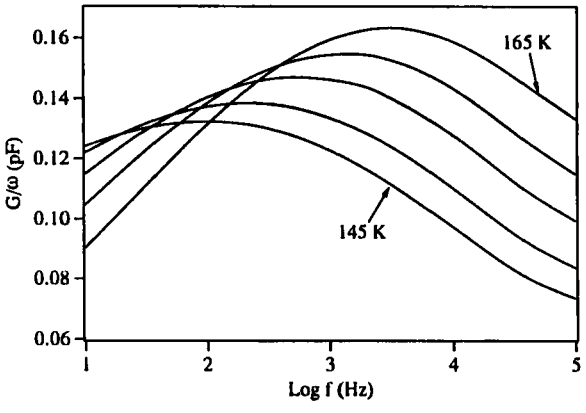

FIGURE 2 Dielectric loss spectrum of the low-temperature γ-process in the unaligned C7DP8 from 145 K to 165 K with 5 K increment.

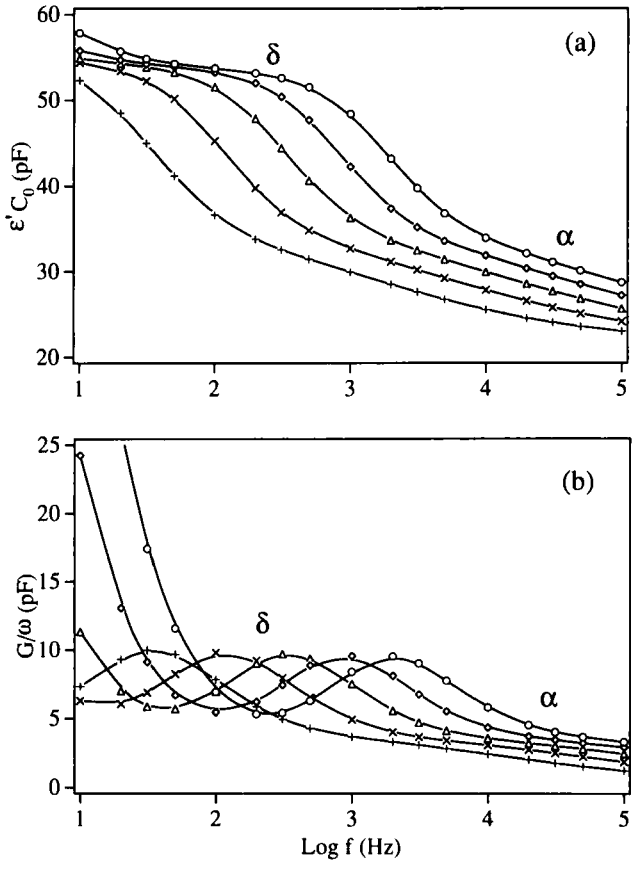

FIGURE 3 δ and α processes of the unaligned C7DP8 in the smectic-A (s_A) phase (+310 K, ×315 K, △320 K, ◇325 K, ○330 K). (a) Real part—capacitance $\varepsilon' C_0$; (b) imaginary part—dielectric loss G/ω.

process which requires the accurate determination of the relaxation frequency, ω_R or f_R (relaxation time $\tau_R = 1/\omega_R$), at a given temperature.[10,37]

The Fuoss-Kirkwood function, a symmetric empirical lineshape, has been used to fit the spectra to get the necessary information by means of nonlinear least-squared minimization method (Levenberg-Marquardt).[37] In the temperature range from 295–350 K where the samples are in s_A phase, the dielectric loss spectra, $L(\omega)$ or $[G(\omega)/\omega]$, are thought to consist of a low-frequency δ peak, a high-frequency α peak, and a DC conductance. The data is fitted with two Fuoss-Kirkwood functions plus a DC conductivity (σ_{DC}) term.

$$L(\omega) = (G_{DC}/\omega) + \sum_{\delta,\alpha} A_i \,\mathrm{Sech}[\beta_i \ln(\omega/\omega_{Ri})] \tag{2}$$

Alternatively, with $\omega = 2\pi f$ and Equation (1), the normalized loss spectra are,

$$\varepsilon''(\omega) = (\sigma_{DC}/2\pi f \varepsilon_0) + \sum_{\delta,\alpha} \varepsilon''_{mi} \,\mathrm{Sech}[2.303\beta_i \log_{10}(f/f_{Ri})] \tag{3}$$

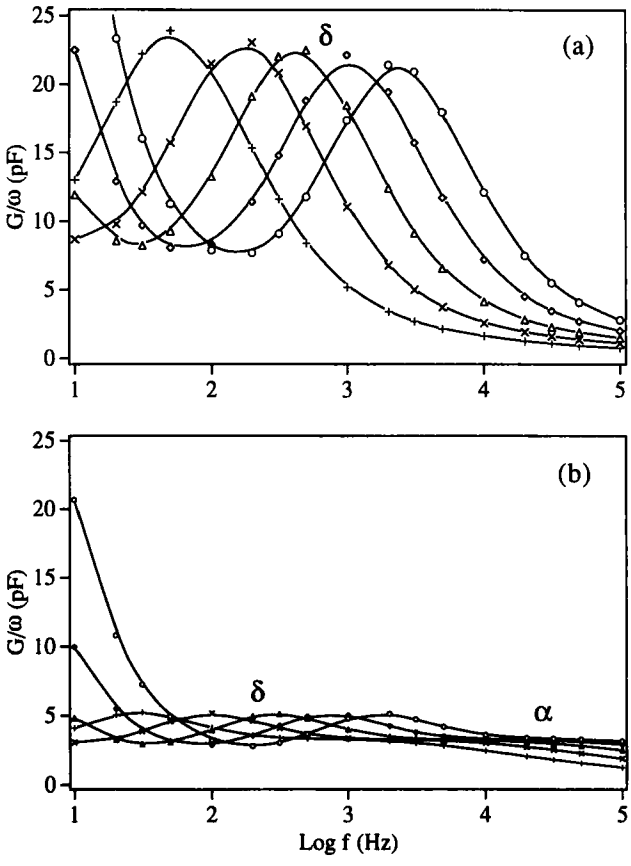

FIGURE 4 Dielectric loss spectra for the aligned C7DP8 from 310 K–330 K (+310 K, ×315 K, △320 K, ◇325 K, ○330 K). (a) Homeotropic (H); (b) planar (P) or homogeneous.

where, A and ε''_m are respectively loss amplitude and the amplitude of the imaginary part of the complex dielectric constant; β lies between 0 and 1 and is a width distribution parameter and equals to 1.14/(width of loss peak at half-height). The Fuoss-Kirkwood function reduces to a Debye-type when $\beta = 1$. The dielectric relaxation strength for each process, $\Delta\varepsilon'$, the difference in the dielectric constants at low-end and high-end frequencies and proportional to the amount of dipole moments involved in the relaxation, can be expressed in terms of two fitting parameters,[10]

$$\Delta\varepsilon' \equiv \varepsilon'_0 - \varepsilon'_\infty = 2\varepsilon''_m/\beta. \tag{4}$$

Figure 5 demonstrates the fitting process in which the normalized loss ($G/\omega C_0$) of the unaligned C7DP30 at 320 K has been fitted to a DC conductivity, $\sigma_{DC} = 4.5 \times 10^{-2}$ S/m, and two Fuoss-Kirkwood lineshapes representing the δ and α peaks, [see Equation (3)]. This fitting process has been employed to all the samples in the s_A region from 300–350 K and Table II summarizes the results at 320 K as well as the calculated dielectric strengths [Equation (4)]. C7DP8 has a DC con-

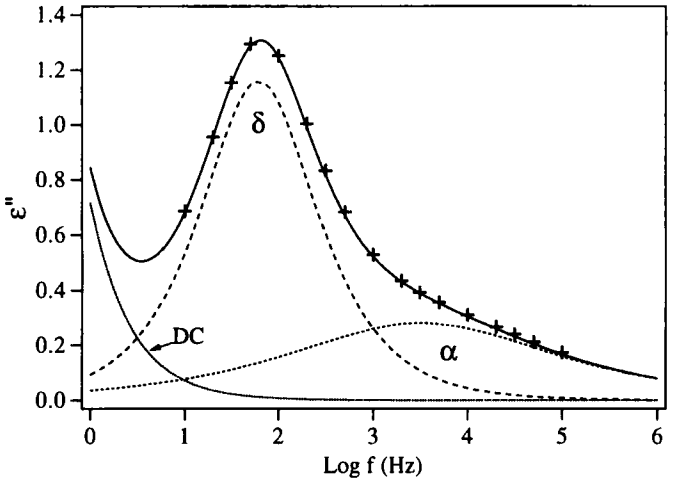

FIGURE 5 The normalized loss ($G/\omega C_0$, +) of the unaligned C7DP30 fitted into a DC conductivity, $\sigma_{DC} = 4.5 \times 10^{-12}$ S/m, and two Fuoss-Kirkwood lineshapes (dashed curves) according to Equation (3). The solid curve represents a superposition of the three dashed curvatures.

TABLE II

Results from Fuoss-Kirkwood data fitting for all the studied samples at 320 K

Sample	Align.	σ_{DC}	δ-peak				α-peak			
		(10^{-12}S/m)	$\log f_R$	ε''_m	β	$\Delta\varepsilon'$	$\log f_R$	ε''_m	β	$\Delta\varepsilon'$
C7DP8	U-	86	2.53	1.17	0.85	2.76	4.29	0.39	0.34	2.25
	H-	90	2.64	3.19	0.82	7.75	--	--	--	--
	P-	35	2.42	0.50	0.94	1.07	4.17	0.43	0.33	2.56
C7DP30	U-	4.5	1.79	1.16	0.78	2.98	3.51	0.28	0.34	1.68
	H-	8.7	1.83	2.62	0.83	6.32	3.38	0.15	0.32	0.97

ductivity nearly one order of magnitude larger than C7DP30 probably due to the shorter chain length resulting in a relatively small viscosity and high mobility. The deviation in DC conductivities in different alignments for each sample may be due to the different mobilities of ions in various orientations.

DISCUSSION

δ-Relaxation

The individual dielectric relaxation processes in this paper will be assigned in terms of the rotational diffusion mode theory[10,28,29] according to the loss spectra in the

different macroscopic orientations. The longitudinal component of the dipole moment in the side-chain mesogen, μ_l, is approximately 5 Debye, which comes from its cyano-biphenyl end-group (—C≡N), and is much larger than the transverse component, μ_t, approximately 2 Debye from the oxy-group (—O—). The fact that the δ-peaks are much stronger than the α-peaks (Figures 3 and 4) implies that the stronger dipole moments are involved in this process, mainly μ_l. As mentioned before, the δ-peak is enhanced in the H-alignment and is suppressed in the P-alignment at a certain temperature as compared with the unaligned sample, e.g., the dielectric relaxation strength $\Delta\varepsilon'$ is 7.75 in the H-aligned C7DP8, 1.07 in the P-alignment, and 2.76 in the unaligned sample (see Table II), which suggests an involvement by the longitudinal component μ_l since μ_l is along the easy-optical axis in the uniaxial LC. Because the width parameter β is close to 1, the δ-peak is mainly associated with only one single mode, hence it is a Debye-like process.[10] It follows that the low-frequency δ-peak can be assigned to the 180° rotation of the longitudinal dipole moment in the mesogenic group about its short axis, in smectic-A phase, it is possible for the side group to flip around the polymer backbone, hopping from one smectic layer to another.

The dielectric relaxation frequency in the δ process at a given temperature is almost independent of the alignment configuration, for instance about 316 Hz for C7DP8 at 320 K, in light of local-ordering in LC polymer system.[16,19] However, the polymer chain length or molecular weight does affect the relaxation of the mesogen so that the longer chain length with its higher T_g and higher viscosity produces a lower relaxation rate. On the average, the longer chain C7DP30 has a relaxation frequency about $10^{0.8}$ Hz lower than the shorter chain C7DP8 at the same temperature, which clearly indicates that the longer polymer backbone hinders the rotation of the mesogen about its short axis and also makes β slightly smaller in amplitude than the shorter chain sample.

The loss amplitude in the H-aligned sample decreases slowly with increasing temperature, see Figure 4(a), which may result from the deviation of the LC director (the long axis of the molecule, or the easy-optical axis) from the layer normal due to the increasing thermal fluctuations with increasing temperature.

α-Relaxation

The weak high-frequency α-peaks are observed in the unaligned samples (Figure 3), while they are enhanced in the P-alignment and are almost absent in the H-alignment (see Figure 4 and Table II). The average width parameter β is about 0.33 and roughly independent of the chain length, therefore, this process can be thought to involve both longitudinal and transverse dipole moments in the mesogenic group which combine into a few different rotational modes. Since the amplitudes of the α-peaks are much smaller than those of the δ-peaks and almost uncoupled with the driving electric field in the H-aligned samples, the major contribution to the α process comes from the transverse dipole moments ($\mu_t < \mu_l$) rotating about their long axis. Being similar to the δ process, the relaxation frequency in the α process of each sample in the isothermal condition remains nearly unchanged independent of the alignment and is slowed down by $10^{0.8}$ Hz from C7DP8 to C7DP30.

Glassy Behaviors

The loss-maxima frequencies vs. reciprocal temperature (Arrhenius plot) in the both δ and α processes display curved, non-Arrhenius behaviors and the relaxation frequencies decrease rapidly as the temperature approaches T_g in the mesophase region (see Figure 6 for C7DP8), which demonstrates typical glassy behaviors in the polymeric materials. The activation energy for the δ process at 320 K is around 153 kJ/mole for C7DP8, 218 kJ/mole for C7DP30. The α process has a similar activation energy but deviates from the δ process as T approaches T_g. The activation energies in both δ and α processes increase rapidly as T approaches T_g. Although this kind of glassy behavior is performed by the mesogenic group in the side-chain, which is connected to the polymer backbone via seven carbon spacers, it must represent the polymer's structural motion to some extent. In other words, some information regarding the polymer backbone's motion near T_g may be provided by monitoring the relaxations in the side-chain. It is of fundamental interest to understand the debated glass transitions in the polymeric materials.[31,38]

Two phenomenological equations, WLF and VF equations, given in the following, have been used to study the glassy behaviors in the δ- and α- relaxations.

WLF equation,

$$\mathrm{Log}_{10}[f_R(T)/f_R(T_0)] = A(T - T_0)/(B + T - T_0) \tag{5}$$

where, A and B can take the universal values, $A = 8.66$, $B = 101.6$, when $T_0 = T_g + 50$ K. This equation basically gives the relation between the relaxation frequency and the glass transition in most polymeric materials.

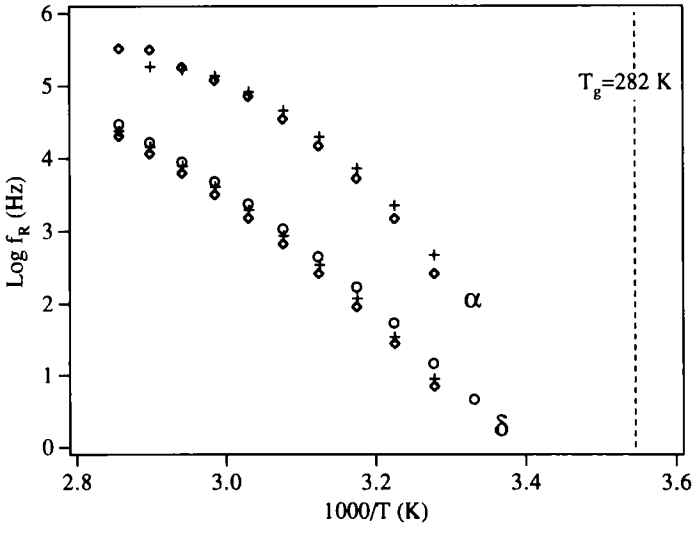

FIGURE 6 Arrhenius plot for the δ and α processes in C7DP8 (+ unaligned, ○ H-aligned, ◇ P-aligned). Note, the α process is absent in the H-aligned sample.

VF equation,

$$f_R = f^0 \exp[-C/(T - T_\infty)] \tag{6}$$

where, f^0 is very high usually between 10^{10} Hz and 10^{12} Hz, may also be a polynomial function of temperature; T_∞ is sometimes called Vogel temperature with $T_\infty < T_g$.

Figure 7 demonstrates the δ- and α-processes in the P-aligned C7DP8 being fitted to either WLF or VF equations and Table III lists all the results for the studied samples. The WLF results can be verified by inspecting the consistency between

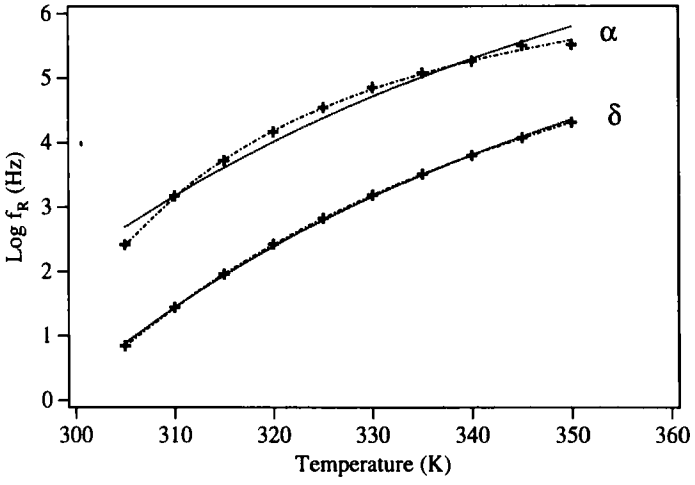

FIGURE 7 The δ and α processes of the P-aligned C7DP8 fitted by WLF and VF equations. +, relaxation frequencies; ·····, WLF fitting; –·–·–, VF fitting.

TABLE III

Results from WLF and Vogel-Fulcher equations for two major relaxation processes of all studied samples, (f and f^0 in Hz; T_0, C, and T_∞ in K)

		WLF				Vogel-Fulcher					
Sample	Align.	δ		α		δ			α		
		logf(T_0)	T_0	logf(T_0)	T_0	$\log f^0$	C	T_∞	$\log f^0$	C	T_∞
C7DP8	U-	2.45	320	3.34	310	9.11	1159	243	6.99	240	281
	H-	2.36	317	--	--	10.4	1721	224	--	--	--
	P-	2.37	320	3.53	314	9.54	1361	237	7.64	351	276
C7DP30	U-	2.78	331	3.60	322	6.83	586	270	5.05	84.7	297
	H-	2.22	325	2.68	310	8.99	1188	248	10.5	1620	221

$f_R(T_0)$ and T_0, i.e., $f_R(T_0)$ should be the relaxation frequency at temperature T_0. For example, $\log f_R(310\text{ K})$ for the a process of the unaligned C7DP8 is, respectively, 3.34 from the WLF equation (5) and 3.35 from the direct loss peak finding. In C7DP8, the relaxation frequency average $10^{0.8}$ Hz higher than C7DP30 roughly equals to 8 K difference in T_g, which is consistent with the DSC measurement (see Table I). Figure 8 shows the δ-relaxation frequency vs. "normalized temperature" $(T - T_g)/T_g$ for both the shorter chain C7DP8 and the longer chain C7DP30. The WLF equation (5) fits them very well and both C7DP8 and C7DP30 have the similar glassy nature, independent of the polymer chain length. However, the WLF calculated glass transition T_g^{WLF} ($= T_0 - 50$ K) is 12–22 K lower than the calorimetric T_g for C7DP8 and 10–30 K lower for C7DP30. On the other hand, the glass transition of poly{vinyl methyl ether} (PVME),[34] T_g^{PVME}, is at 245 K, about 37 K and 45 K lower than our polyvinyl-ether based C7DP8 and C7DP30, respectively. The T_g^{WLF} is allocated in the range between T_g^{PVME} and the SCLCP glass transition temperature T_g^{SCLCP}, which implies that the glassy behavior in the SCLCP system may result from the cooperative motion between the side-chain and the polymer backbone. The observed glassy behavior of the side-chain mesogen, therefore, also reflects the structural cooperative motion of the polymer main chain to some extent. In the VF [Equation (6)] results, the frequency prefactor f^0 is far smaller than the universal value 10^{12} Hz and f^0 should have been treated as a polynomial function of temperature. The Vogel temperature T_∞ is overall below the calorimetric T_g for both δ and α processes in all the studied samples, except for the α process in the unaligned C7DP30, which has fewer data points.

Dielectric Anisotropy

The dielectric anisotropy, ε_a, is defined as the difference between dielectric constants when the LC director is parallel to the external electric field and when it is

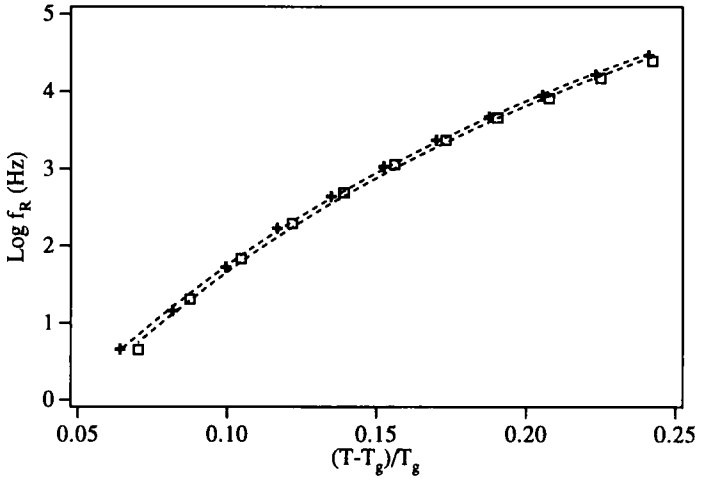

FIGURE 8 δ-relaxation frequency vs. "normalized temperature" $(T - T_g)/T_g$. +, C7DP8 (T_g = 282 K); □, C7DP30 (T_g = 290 K); - - - - - - -, WLF fitting.

perpendicular to the field, i.e., the dielectric constant difference between the H-alignment and the P-alignment,[39]

$$\varepsilon_a \equiv \varepsilon'_{\parallel} - \varepsilon'_{\perp} \tag{7}$$

Figure 9(a) plots the $\varepsilon'_{\parallel}$ and $\varepsilon'_{\perp}$ of C7DP8 vs. log frequency at 320 K with a crossover $f_c = 1.6$ kHz. The sample has a positive dielectric anisotropy, $\varepsilon_a > 0$ for $f > f_c$ and exhibits a negative anisotropy, $\varepsilon_a < 0$, for $f > f_c$. Figure 9(b) shows the crossover frequency f_c vs. temperature and log f_c is in a near linear increase with temperature. The sample favors H-alignment when a low-frequency AC electric field is applied while it favors P-alignment if a high-frequency field is applied. From this point of view, using two-frequency addressing technique,[16,40] the sample can also be aligned into H- or P-states when it is cooled down from its isotropic temperature to room temperature under intensive AC electric fields. However, in our cyano-biphenyl samples, the positive anisotropy $\varepsilon_a(f < f_c)$ is much larger than the negative anisotropy $\varepsilon_a(f > f_c)$ and it is expected that the H-alignment could be obtained while the P-alignment would be very difficult to be achieved by AC electric fields.

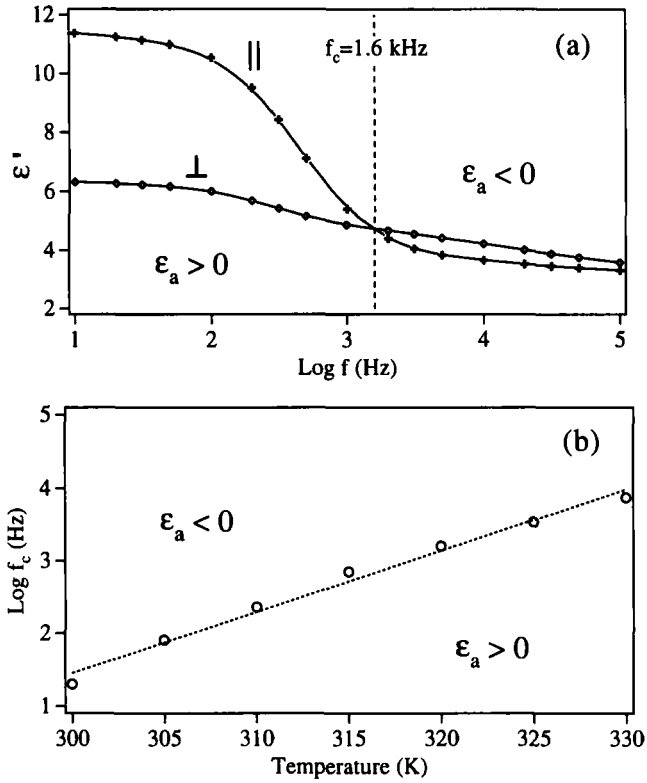

FIGURE 9 Dielectric anisotropy ε_a in C7DP8, (a) $\varepsilon'_{\parallel}$ and $\varepsilon'_{\perp}$ at 320 K with crossover frequency f_c = 1.6 kHz; (b) f_c varying with temperature, nearly an exponential relation.

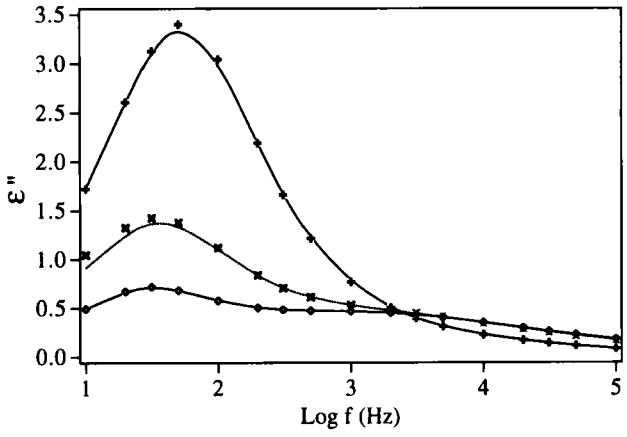

FIGURE 10 ε'' spectra of C7DP8 at 310 K ($\times$ ε''_U, + ε''_H, $\diamond$ ε''_P). The dashed curve is a result of Equation (9) with $S_d = -0.125$.

Director Order Parameter

The director order parameter S_d, between -0.5 and 1.0, can be used to evaluate the degree of alignment in the SCLCP system, assuming that S_d is 1 in the perfect H-alignment, -0.5 in the ideal P-alignment, 0 in the absolutely unaligned sample. Attard, Araki, and Williams[19] suggested that S_d can be expressed as

$$S_d = \frac{2(G/\omega)_U - [(G/\omega)_H + 2(G/\omega)_P]}{2[(G/\omega)_H - (G/\omega)_P]} \tag{8}$$

Alternatively,

$$\varepsilon''_U(\omega) = (1 + 2S_d)\varepsilon''_H(\omega)/3 + 2(1 - S_d)\varepsilon''_P(\omega)/3 \tag{9}$$

where, subscripts U, H, and P stand for unknown or "unaligned," H-alignment, and P-alignment, respectively.

Figure 10 shows the spectra of the unaligned, H-aligned, and P-aligned C7DP8 at 310 K. The S_d for the "unaligned" sample is -0.125 from fitting Equation (9), which indicates that our "unaligned" C7DP8 shows some H-alignment and LC molecules tend to be perpendicular to the glass plates without any alignment efforts although such tendency is rather weak.

CONCLUSION

Two major relaxation processes in the polyvinyl-ether based cyano-biphenyl side-chain liquid-crystalline polymers have been confirmed in terms of the rotational diffusion mode theory in comparisons of the unaligned, homeotropically and planarly aligned samples in smectic-A phase. The glassy behaviors of these two relaxations near T_g investigated by WLF and Vogel-Fulcher equations may also have

some correlations with the polymer backbone. The polymer chain length only affects the relaxation frequency and basically does not change the nature of the specific relaxation process. The strong positive dielectric anisotropy in such a system suggests that the samples can be homeotropically aligned in a presence of a low-frequency AC electric field.

Acknowledgment

We are very grateful to Prof. Charles Rosenblatt for his generous assistance in the use of the superconducting magnet and Prof. Rolfe Petschek, D. Gu and M. Lee for their helpful discussions. This work was supported by NSF/MRG Grant DMR 89-01845. Partial support for Z. Z. Z. by NSF/S&TC Advanced Liquid Crystalline Optical Materials (ALCOM) under Grant DMR 89-20147 is also gratefully acknowledged.

References

1. H. Finkelmann, M. Portugall and H. Ringsdorf, *Am. Chem. Soc., Div. Polym. Chem.*, **19**, 183 (1978); H. Finkelmann, D. Naegele and H. Ringsdorf, *Makromol. Chem.*, **180**, 803 (1979).
2. N. A. Plate and V. P. Shibaev, *Comb-Shaped Polymers and Liquid Crystals* (Plenum Press, New York, 1987), Chap. 4, pp. 199–415.
3. M. Engel, B. Higen, R. Keller, W. Kreuder, B. Reck, H. Ringsdorf, H.-W. Schmidt and P. Tschirner, *Pure & Appl. Chem.*, **57**, 1009 (1985).
4. V. Percec and C. Pugh, in *Side Chain Liquid Crystal Polymers* (Chapman, New York, 1989), C. B. McArdle, Ed., Chap. 3, pp. 30–105.
5. C. B. McArdle, *ibid*, Chap. 1, pp. 1–6.
6. C. Noël, *ibid*, Chap. 6, pp. 159–195.
7. C. B. McArdle, *ibid*, Chap. 13, pp. 357–394.
8. G. R. Möhlmann and C. P. J. M. van der Vorst, *ibid*, Chap. 12, pp. 330–356.
9. W. Haase, *ibid*, Chap. 11, pp. 309–329.
10. C. M. Haws, M. G. Clark and G. S. Attard, *ibid*, Chap. 7, pp. 196–223.
11. V. V. Daniel, *Dielectric relaxation* (Academic Press, London, 1967), Chaps. 6, 7, & 14.
12. H. Kresse and R. V. Talrose, *Makromol. Chem., Rapid Commun.*, **2**, 369 (1981); H. Kresse, S. Kostromin and V. P. Shibaev, *ibid*, **3**, 509 (1982); H. Kresse and V. P. Shibaev, *ibid*, **5**, 63 (1984).
13. H. Kresse, A. Wiegeleben and B. Krucke, *Acta Polymerica*, **39**, 583 (1988).
14. H. Kresse, S. Ernst, B. Krucke, F. Kremer and S. U. Vallerien, *Liq. Cryst.*, **11**, 439 (1992).
15. G. S. Attard, G. Williams, G. W. Gray, D. Lacey and P. A. Gemmel, *Polymer*, **27**, 185 (1986).
16. G. S. Attard and G. Williams, *Liq. Cryst.*, **1**, 253 (1986).
17. G. S. Attard, *Molecular Phys.*, **58**, 1087 (1986).
18. G. S. Attard, J. J. Moura-Ramos and G. Williams, *J. Polym. Sci.*, **B25**, 1099 (1987).
19. G. S. Attard, K. Araki and G. Williams, *Brit. Polym. J.*, **19**, 119 (1987).
20. J. J. Moura-Ramos and G. Williams, *Polymer*, **32**, 909 (1991).
21. G. Williams, A. Nazemi, F. E. Karasz, J. S. Hill, D. Lacey and G. W. Gary, *Macromolecules*, **24**, 5134 (1991).
22. H. Pranoto, F.-J. Bormuth and W. Haase, *Makromol. Chem.*, **187**, 2453 (1986); F.-J. Bormuth and W. Haase, *Mol. Cryst. Liq. Cryst.*, **148**, 1 (1987); F.-J. Bormuth and W. Haase, *Liq. Cryst.*, **3**, 881 (1988).
23. R. Zentel, G. R. Strobl and H. Ringsdorf, *Macromolecules*, **18**, 960 (1985).
24. C. M. Haws, M. G. Clark and C. B. McArdle, *Mol. Cryst. Liq. Cryst.*, **153**, 537 (1987).
25. H. Seiberle, W. Stille and G. Strobl, *Macromolecules*, **23**, 2008 (1990).
26. L. Monnerie, F. Lauprêtre and C. Noël, *Liq. Cryst.*, **3**, 1013 (1988).
27. G. Meier and A. Saupe, *Molec. Crystals*, **1**, 515 (1966).
28. P. L. Nordio, G. Rigatti and U. Segre, *Molec. Phys.*, **25**, 129 (1973).
29. P. L. Nordio and U. Segre, in *The Molecular Physics of Liquid Crystals* (Academic Press, New York, 1979), G. R. Luckhurst and G. W. Gray, Eds., Chap. 18, pp. 411–426.
30. X.-J. Wang and M. Warner, *Phys. Letts.*, **A119**, 181 (1986); X-J. Wang and M. Warner, *J. Phys.* **A20**, 713 (1987).

31. W. Götze, in *Liquids, Freezing and Glass transition* (North-Holland, Amsterdam, 1991), J. P. Hansen, D. Levesque and J. Zinn-Justin, Eds., Course 5, pp. 287–503.
32. V. Percec and M. Lee, *Macromolecules*, **24**, 1017 (1991); V. Percec and M. Lee, *Macromolecules*, **24**, 2780 (1991); V. Percec, M. Lee, and H. Jonsson, *J. Polym. Sci.*, **A29**, 327 (1991).
33. C. G. Andeen, *Ph.D. Thesis* (Case Western Reserve University, Cleveland, 1971), unpublished.
34. K. Pathmanathan and G. P. Johari, *J. Polym. Sci.*, **B25**, 379 (1987).
35. G. D. Smith, F. Liu, R. W. Devereux and R. H. Boyd, *Macromolecules*, **25**, 703 (1992).
36. H. R. Zeller, *Phys. Rev. A*, **23**, 1434 (1981); H. R. Zeller, *Phys. Rev. Lett.*, **48**, 334 (1982).
37. R. B. Akins, *Ph.D. Thesis* (Case Western Reserve University, Cleveland, 1991), unpublished.
38. E. W. Fisher, E. Donth and W. Steffen, *Phys. Rev. Lett.*, **68**, 2344 (1992).
39. P. G. de Gennes, *The Physics of Liquid Crystals* (Clarendon Press, Oxford, London, 1975), pp. 95–97.
40. G. S. Attard, K. Araki and G. Williams, *J. Mol. Electr.*, **3**, 1 (1987).